

**Supporting Information for**

**Photohole-Oxidation-Assisted Anchoring of Ultra-Small Ru Clusters onto  
TiO<sub>2</sub> with Excellent Catalytic Activity and Stability**

**Changming Li,<sup>a</sup> Shitong Zhang,<sup>a</sup> Bingsen Zhang,<sup>b</sup> Dangsheng Su,<sup>b</sup> Shan He,<sup>a</sup> Yufei Zhao,<sup>a</sup> Jie  
Liu,<sup>a</sup> Fei Wang,<sup>a</sup> Min Wei,<sup>\*a</sup> David G. Evans<sup>a</sup> and Xue Duan<sup>a</sup>**

<sup>a</sup> *State Key Laboratory of Chemical Resource Engineering, Beijing University of Chemical  
Technology, Beijing 100029, P. R. China*

<sup>b</sup> *Shenyang National Laboratory of Materials Science, Institute of Metal Research, Chinese  
Academy of Sciences, Shenyang 110016, P. R. China*

\* Corresponding author. Tel: +86-10-64412131; Fax: +86-10-64425385.

E-mail address: [weimin@mail.buct.edu.cn](mailto:weimin@mail.buct.edu.cn).

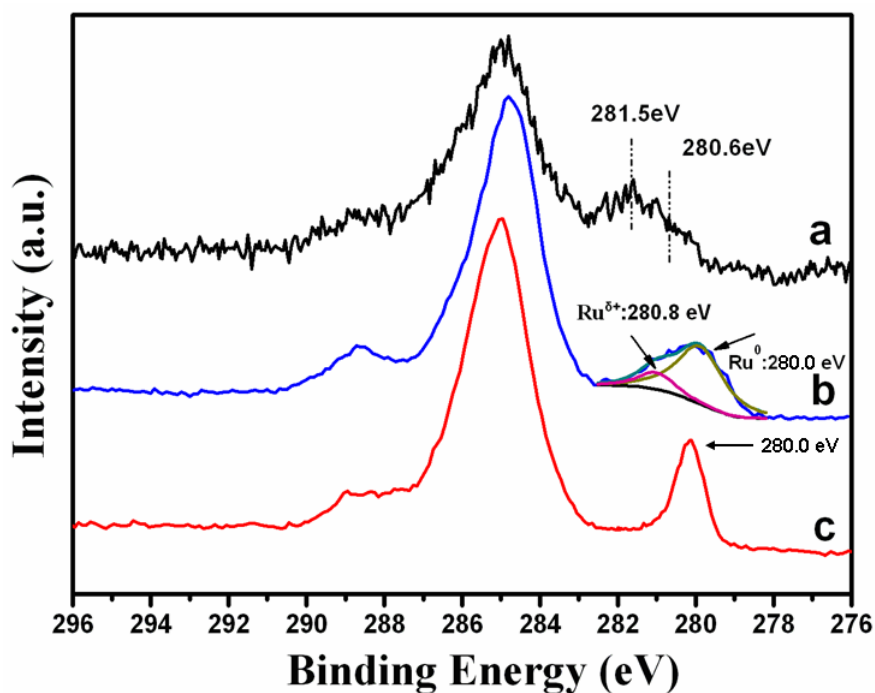


**Figure S1.** Ru 3d<sub>5/2</sub> XPS profiles of (a) the RuO<sub>2</sub>/TiO<sub>2</sub>(PO) sample obtained by photoirradiation, (b) the Ru/TiO<sub>2</sub>(PO), (c) the Ru/TiO<sub>2</sub>(IMP) sample.

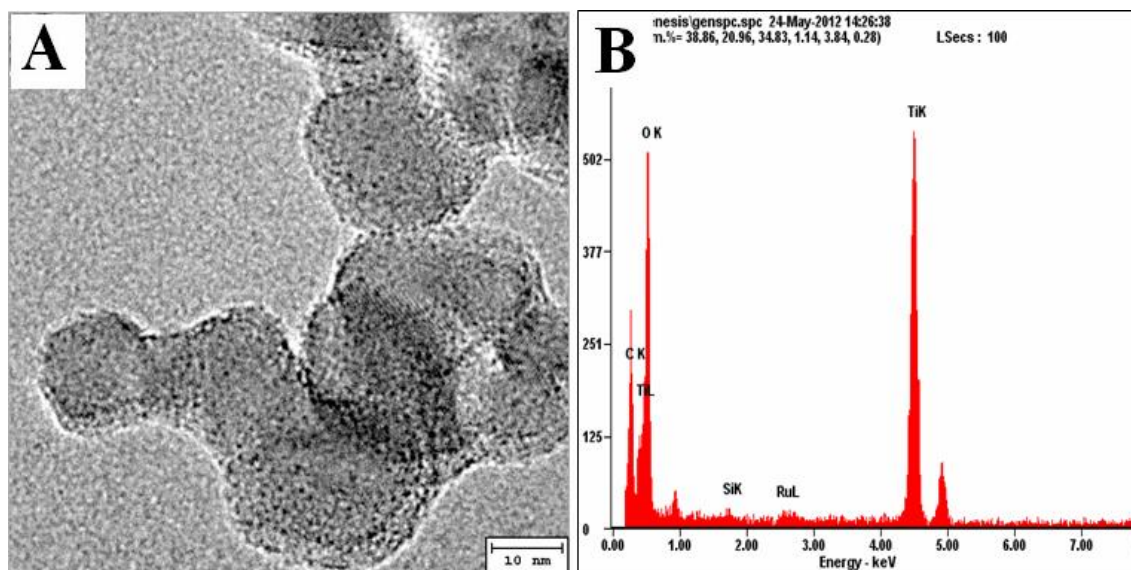


**Figure S2.** TEM image (A) and EDS spectrum (B) of RuO<sub>2</sub>/TiO<sub>2</sub>(PO) obtained by photoirradiation. The size of the small dots is below 0.8 nm; the EDS spectrum confirms the presence of Ru species loaded on TiO<sub>2</sub>.

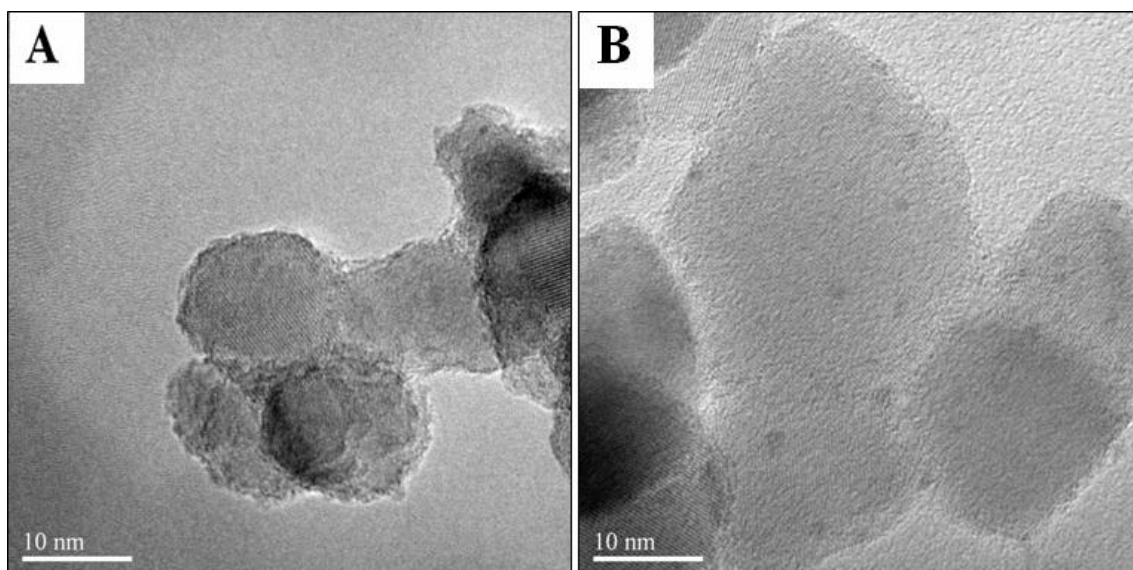


**Figure S3.** TEM images of (A) the sample prepared under the same conditions as the photohole-assisted method except with the absence of UV-radiation, (B) after reduction of (A) in hydrogen atmosphere at 400 °C.

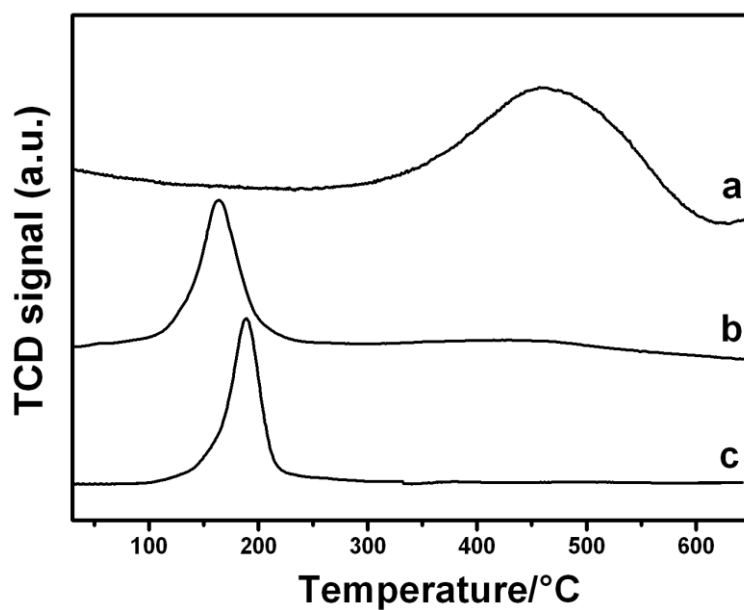


**Figure S4.** Hydrogen temperature programmed reaction (H<sub>2</sub>-TPR) profiles of (a) RuO<sub>2</sub>/TiO<sub>2</sub>(PO), (b) RuO<sub>2</sub>/TiO<sub>2</sub>(IMP), (c) crystalline RuO<sub>2</sub>.

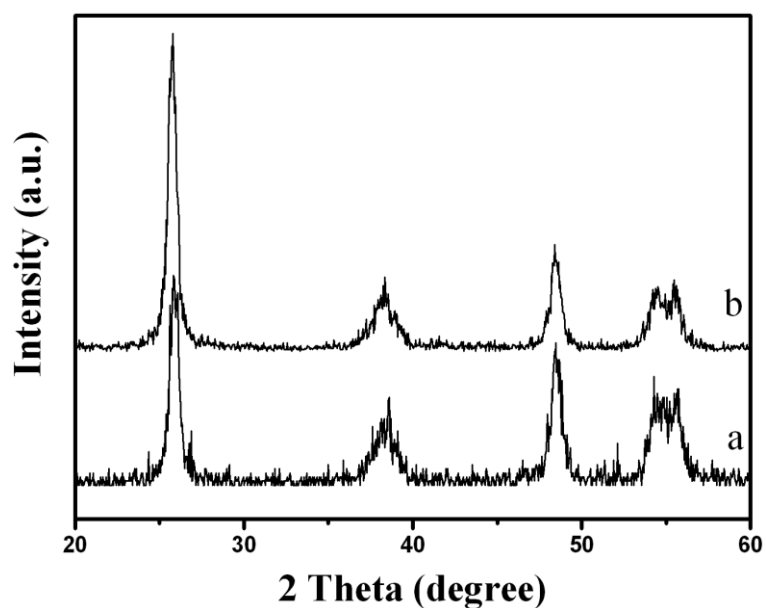


**Figure S5.** XRD patterns of (a)  $\text{RuO}_2/\text{TiO}_2(\text{PO})$ , (b)  $\text{Ru}/\text{TiO}_2(\text{PO})$ . No reflection of  $\text{RuO}_2$  or Ru species was found for  $\text{RuO}_2/\text{TiO}_2(\text{PO})$  or  $\text{Ru}/\text{TiO}_2(\text{PO})$ , implying  $\text{RuO}_2$  or Ru species with a rather small particle size was loaded on  $\text{TiO}_2$  by using the photohole-oxidation-assisted anchoring method.

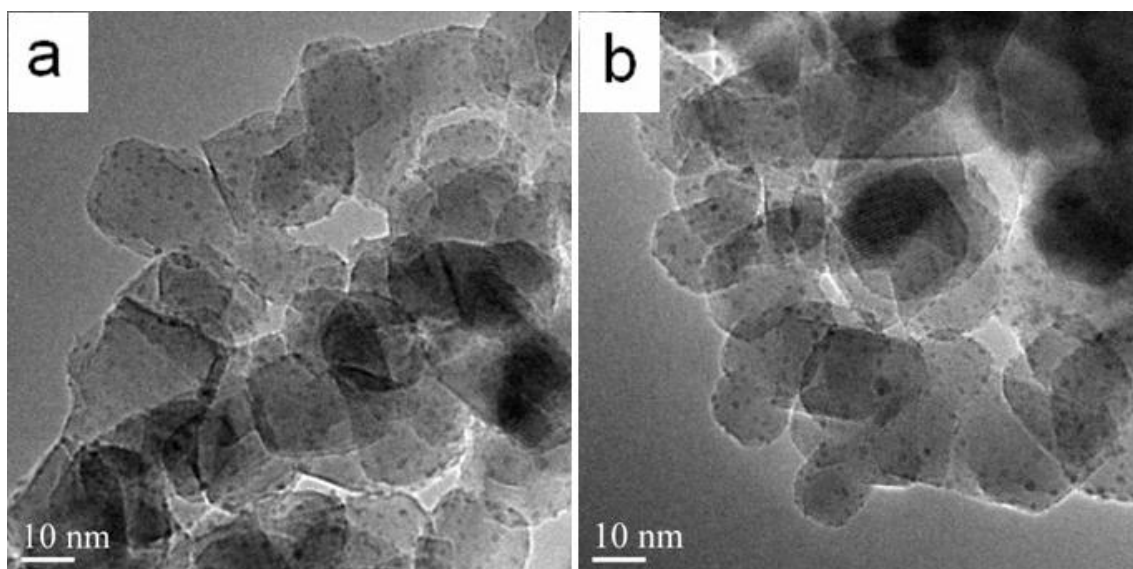


**Figure S6.** TEM images of  $\text{Ru}/\text{TiO}_2(\text{PO})$  samples after calcination in a  $\text{H}_2$  atmosphere at different temperatures: (a)  $500\text{ }^\circ\text{C}$ , (b)  $600\text{ }^\circ\text{C}$ .

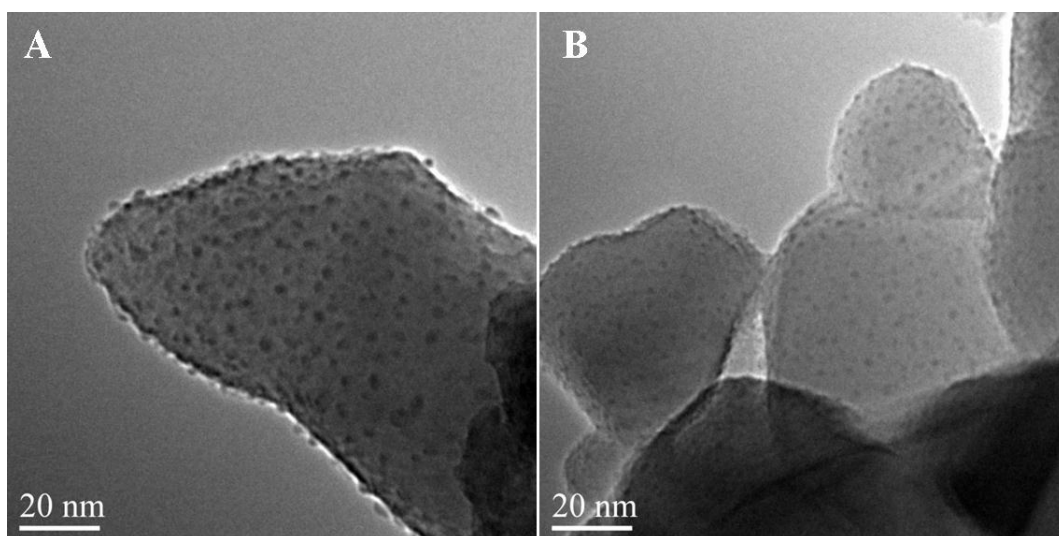


**Figure S7.** Metal-semiconductor materials with high dispersion prepared by the same photohole-oxidation-assisted method: (A) Ru/CeO<sub>2</sub>, (B) Fe/TiO<sub>2</sub>.

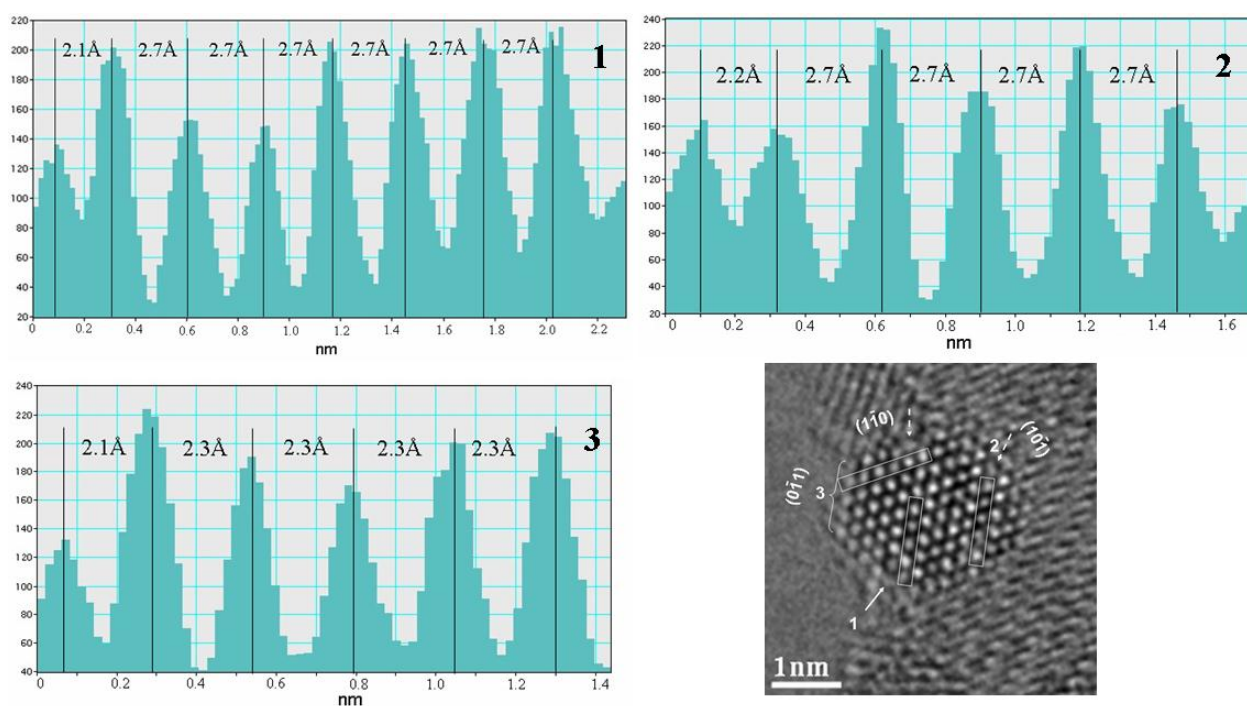


**Figure S8.** Inter-column distance analysis corresponding to Figure 3 in the manuscript: along line 1 in the  $(1\bar{1}0)$  direction, line 2 in the  $(\bar{1}10)$  direction, and line 3 in the  $(10\bar{1})$  direction.

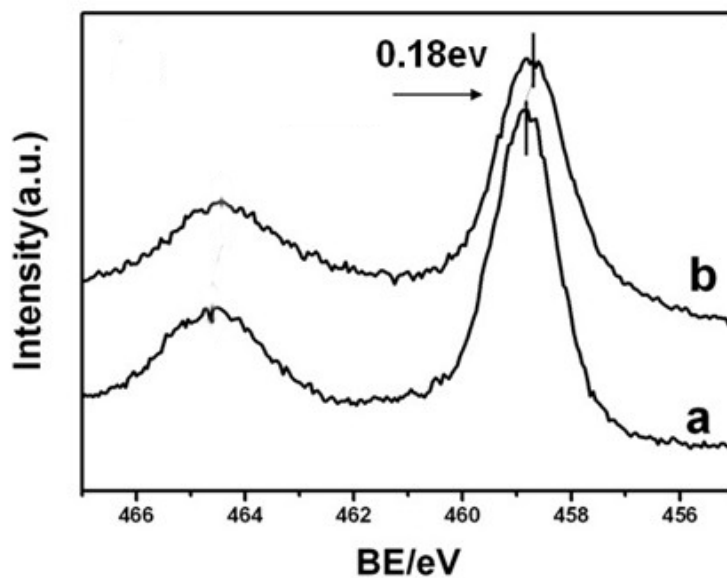


**Figure S9.** Ti 2p XPS profiles for (a) pristine TiO<sub>2</sub> and (b) Ru/TiO<sub>2</sub>(PO). TiO<sub>2</sub> was pretreated under the same conditions as Ru/TiO<sub>2</sub>(PO).

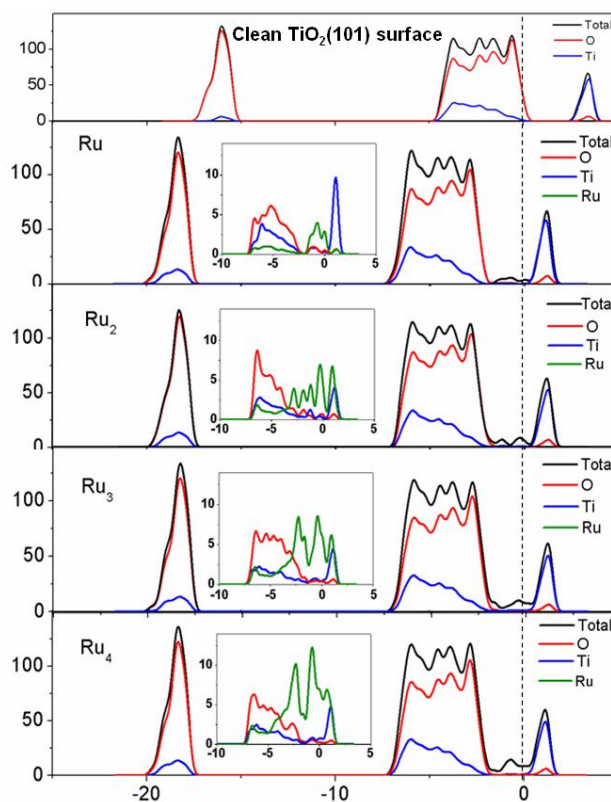


**Figure S10.** Calculated TDOS and LDOS for the pristine TiO<sub>2</sub>(101) surface and a series of Ru<sub>n</sub>-TiO<sub>2</sub> systems. The insets show DOS of Ru as well as of Ti and O atoms neighboring the Ru cluster.

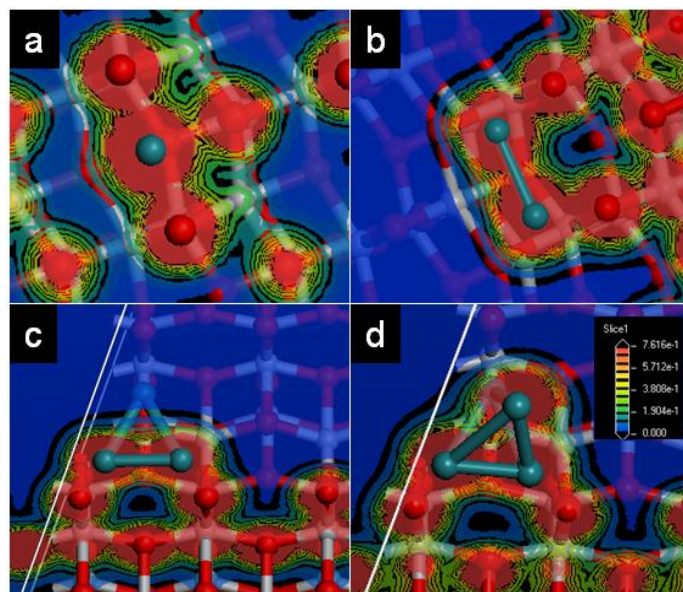


**Figure S11.** Electron density contour maps of the metal–support interface: (a) Ru/TiO<sub>2</sub>, (b) Ru<sub>2</sub>/TiO<sub>2</sub>, (c) Ru<sub>3</sub>/TiO<sub>2</sub> and (d) Ru<sub>4</sub>/TiO<sub>2</sub>. The electron density is in the range 0.0–0.76 e/Å<sup>3</sup>.

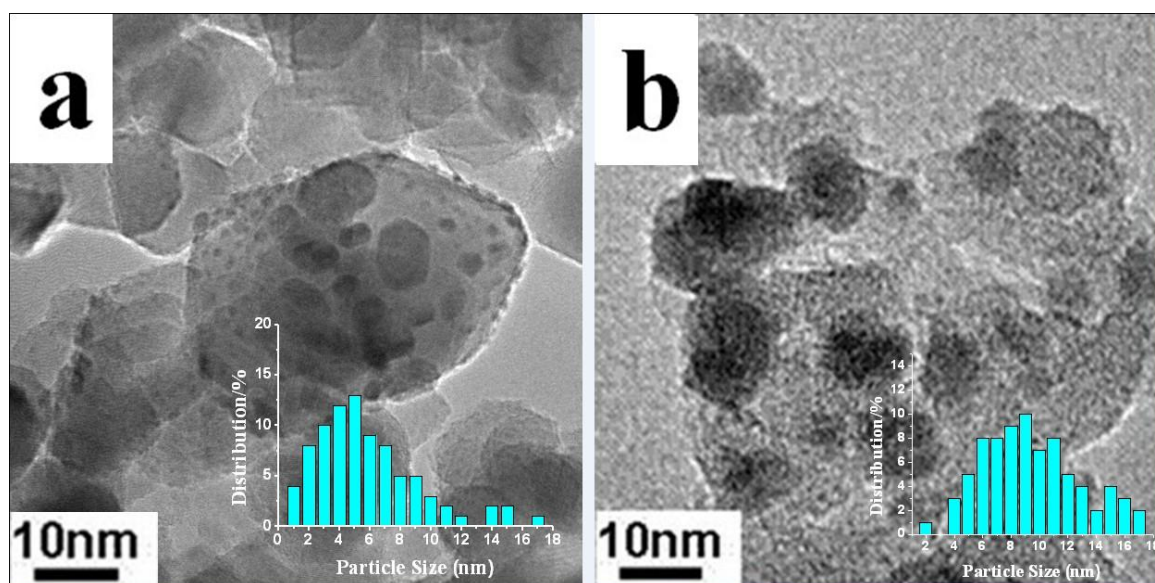


**Figure S12.** TEM images and particle size distribution of (a) Ru/TiO<sub>2</sub>(IMP) and (b) Ru/SiO<sub>2</sub>(IMP). The mean particle size was calculated to be 5.2±0.5 and 9.1±0.8 nm for Ru/TiO<sub>2</sub>(IMP) and Ru/SiO<sub>2</sub>(IMP), respectively.

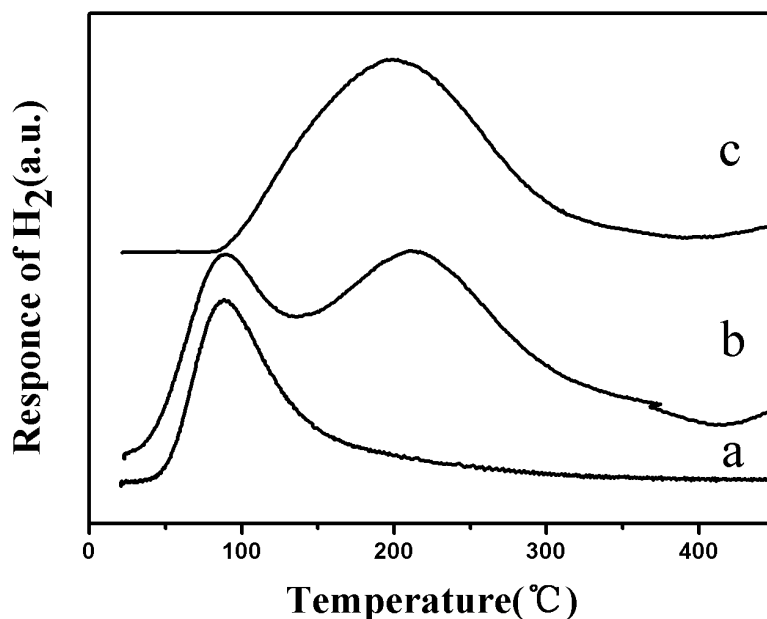


**Figure S13.** Hydrogen temperature programmed desorption ( $\text{H}_2$ -TPD) profiles of (a)  $\text{Ru}/\text{SiO}_2(\text{IMP})$ , (b)  $\text{Ru}/\text{TiO}_2(\text{IMP})$ , (c)  $\text{Ru}/\text{TiO}_2(\text{PO})$ .

### Discussion of density functional theory (DFT) calculations

The optimized geometries of the  $\text{Ru}_n$  ( $n = 1-4$ ) clusters on a  $\text{TiO}_2(101)$  surface with average adsorption energies are shown in Figure 4. Four optimized locations for a single Ru atom adsorbed on anatase  $\text{TiO}_2(101)$  surface were observed (Figure 4: a, b, c and d). When the Ru atom occupies a position between two  $\text{O}_{2c}$  (two-coordinated surface oxygen atoms) in the same row, the structure is the most stable one with an average adsorption energy of 3.59 eV. The Ru atom binds directly to two neighboring  $\text{O}_{2c}$  and two  $\text{O}_{3c}$  (three-coordinated surface oxygen atoms) with an average interatomic distance of 2.08 Å, which results in the weakening of  $\text{Ti}-\text{O}_{3c}$  and  $\text{Ti}-\text{O}_{2c}$  bonds: the  $\text{Ti}-\text{O}_{2c}$  bond is lengthened by 0.1 Å, and  $\text{O}_{3c}$  moves 0.57 Å upward from its equilibrium position, compared with a clean  $\text{TiO}_2(101)$  surface. The  $\text{Ru}_2$  cluster was constructed by adding a Ru atom to the single Ru system and allowing the structure to relax again. The energetically two most favorable

geometries are shown in Figures 4e and 4f. In Figure 4e, it can be seen that each Ru atom simultaneously binds with one  $O_{2c}$  and one  $O_{3c}$  atom, and the average interatomic distances of Ru– $O_{2c}$  and Ru– $O_{3c}$  are 1.99 Å and 2.10 Å, respectively. The  $O_{2c}$  and  $O_{3c}$  atoms respectively move ~0.44 Å and 0.48 Å upward from their equilibrium positions due to the formation of Ru–O bonds. Four geometries of a  $Ru_3$  cluster adsorbed on a  $TiO_2(101)$  surface were taken into consideration in this study (Figure 4: g, h, i and j). The most stable structure of the  $Ru_3$  cluster is presented in Figure 4j, in which an average distance Ru– $O_{2c}$  of 1.96 Å and Ru– $O_{3c}$  of 2.00 Å are obtained, respectively. Moreover, the Ti– $O_{2c}$  bond was lengthened by 0.15 Å. Two stable configurations of a  $Ru_4$  cluster adsorbed on a  $TiO_2(101)$  surface are displayed in Figures 4k and 4l. The average distances of Ru– $O_{2c}$  and Ru– $O_{3c}$  are 2.00 Å and 2.10 Å, respectively. On the basis of the above results, two conclusions can be drawn: (1) the formation of Ru– $O_{2c}$  and Ru– $O_{3c}$  bonds, which results in the weakening of Ti–O bonds, is observed in all these geometries; (2) the surface Ti and Ru atoms do not form a Ti–Ru bond.

To further understand the interaction between Ru and  $TiO_2$  support in terms of electronic structure, the total densities of states (TDOS) as well as the local densities of states (LDOS) of the clean  $TiO_2(101)$  surface and  $Ru_n$ – $TiO_2$  systems were calculated, as shown in Figure S10. For the clean  $TiO_2(101)$  surface, it is found that the valence band (VB) is dominated by O 2p orbitals while the conduction band (CB) is dominated by Ti 3d orbitals, with a calculated band gap of ~3.0 eV. This agrees well with previous reports<sup>1</sup> and confirms the reliability of the calculations. As shown in Figure S10, the band gap disappears as a result of the introduction of Ru: several bands occupy the region from –2.0 eV to 0.5 eV, mainly contributed by Ru 4d orbitals. The DOS of Ti and O atom neighboring with Ru clusters are displayed in the inset illustrations, and also exhibit a distribution

in the range  $-2.0$  to  $0.5$  eV. This can be attributed to the formation of bonding between Ru, O and Ti atoms, resulting in delocalization of the valence electrons of O and Ti atom. To investigate the intrinsic electronic structure at the Ru–TiO<sub>2</sub> interface, the electron densities of these systems were further studied (Figure S11). It was found that the electron densities of both Ru–O and Ti–O bonds are much higher than those of Ti–Ru. The high degree of electron delocalization further indicates that the metal–support interface is predominantly composed of Ru–O and Ti–O bonds, without the formation of metallic Ti–Ru bond.

### References:

- 1 H. G. Yang, C. H. Sun, S. Z. Qiao, J. Zou, G. Liu, S. C. Smith, H. M. Cheng and G. Q. Lu, *Nature*, 2008, **453**, 638.